On-Contact Quenching of 1-Naphtholate by Geminate Protons

Ehud Pines,* Ben-Zion Magnes, and Tamar Barak

Department of Chemistry, Ben-Gurion University of the Negev, P.O.B. 653, Beer −Sheva 84105, Israel

Received: December 15, 2000; In Final Form: July 9, 2001

We have carried out temperature dependence studies of the geminate quenching reaction of 1-naphthol utilizing steady-state and time-resolved fluorescence spectroscopy. The outcome was analyzed using both analytic and numeric procedures. A novel method for estimating the on-contact quenching reaction rate from steady-state quantum-yield measurements is described.

Introduction

Ion pair dynamics are a classic issue in chemical reactivity.[1−3] A related problem is the dynamic branching between self-neutralization and self-quenching[4,5] of electronically excited dyes following proton dissociation. Such photoacids undergo rapid proton dissociation in their electronic excited state, thus providing an efficient mean for creating ion pairs.[6−10] The excited-state photophysics of 1-naphthol, a model photoacid, have been extensively studied in solution over the past 50 years[11−19] following the early observations of photoacidity made by Förster[20] and by Weller.[21]

Pines and Fleming were first to observe the self-quenching reaction of the 1-naphtholate anion by its geminate proton following its excited-state proton dissociation.[4] Since then, the coupled quenching and neutralization geminate recombination reactions of 1-naphthol have attracted considerable theoretical and experimental interest.[5,22−24]

In this study, we show how steady-state quantum-yield measurements of the 1-naphtholate anion may serve to extract the on-contact quenching rate by its geminate proton. The proposed procedure provides a readily available and reliable method for detection and analyzing this important,[4] albeit largely elusive,[12,14,19] feature of the excited-state photophysics of 1-naphthol and its derivatives. To do so, we have developed a set of analytic expressions using simple kinetic arguments, which help to clarify and to highlight the main physical features of this complex kinetic system. The kinetic behavior of 1-naphthol following its excited-state proton dissociation reaction is further verified using a numerical procedure developed by Agmon et al.[9,25] We utilize our method to calculate the temperature dependence of the on-contact quenching rate of 1- naphthol in H_2O and D_2O solvents.

Experimental Section

1-Naphthol was from Sigma (99%+) and was recrystallized from a solution of 10% ethanol with water. H_2O was triple-distilled, and D_2O (99.9% atom purity) was from Aldrich. Absorption spectra were carried out with a HP 8452A diode array spectrometer. The fluorescence spectra were taken with SLM Aminco-Bowman series 2 with *S*/*N* ratio better than 750. The excitation wavelength was at 303.2 nm, which was an isosbestic point, using 2 nm slits for the excitation. The emission of the anion was collected at 470 nm, near the emission peak using 8 nm slits. The pH was adjusted using concentrated HCl (DCl) and NaOH (NaOD) solutions. Figure 1 shows that the ratio between the intensity of the naphtholate anion fluorescence at pH = 12.5 (direct excitation) and its fluorescence intensity at pH = 6.0 (indirect excitation, following the dissociation of the excited naphthol acid) was practically constant between 430 and 650 nm. The intensity ratio between directly (I_{dir}) and indirectly excited (I_{ind}) naphtholate was found to be practically identical to the quantum-yield ratio measured in the two experiments. The ratio was 1.54 at 25 °C and was temperature-dependent (see Results below). Lifetime measurements of the directly excited 1-naphtholate anion were taken by a single-photon counting apparatus, described elsewhere.[5] Excitation and emission wavelengths were 350 and 475 nm, respectively.

Results

Figure 2 shows the temperature dependence of the naphtholate anion fluorescence intensity ratio between 430 and 650 nm when it was excited directly at pH = 12.5 and when it was excited indirectly following the excited-state acid dissociation reaction at pH = 6.0. The ratio was found to decrease with temperature falling from 1.61 at 5 °C to about 1.43 at 55 °C. Similar behavior was found for 1-naphthol in D_2O. In D_2O, the intensities ratio decreased from 1.62 at 5 °C to about 1.48 at 55 °C. The inset in Figure 2 shows that the intensities of both the directly and the indirectly excited 1-naphtholate anion decreased with temperature between 5 and 55 °C (only H_2O data is shown).

The lifetime of the directly excited naphtholate anion was measured at pH = 12.5 and was found to decrease with the temperature between 5 and 55 °C (see Table 1).

Discussion

The quenching of the 1-naphtholate emission at neutral pH's following adiabatic proton dissociation was already observed by the Kuz'min group more than 20 years ago.[19] Kuz'min et al. interpreted their measurements as an indication of solvent quenching. At neutral and basic pH's, the local concentration of the geminate proton far exceeds that of the bulk solution protons during the excited-state lifetime of the naphtholate anion (8.0 ns). The self-quenching reaction may be viewed as a static-like reaction when measured by steady-state fluorescence techniques. Pines and Fleming showed that the diffusion-controlled features of the self-quenching reaction may be time-

* Present sabbatical address: Department of Chemistry, 201 Hildebrand Hall, University of California−Berkeley, Berkeley, CA 94720-1460. Fax: 510-642-6340. Telephone: 510-643-7609. E-mail: epines@zepto.cchem.berkeley.edu.

10.1021/jp0045134 CCC: $20.00
Published on Web 10/03/2001

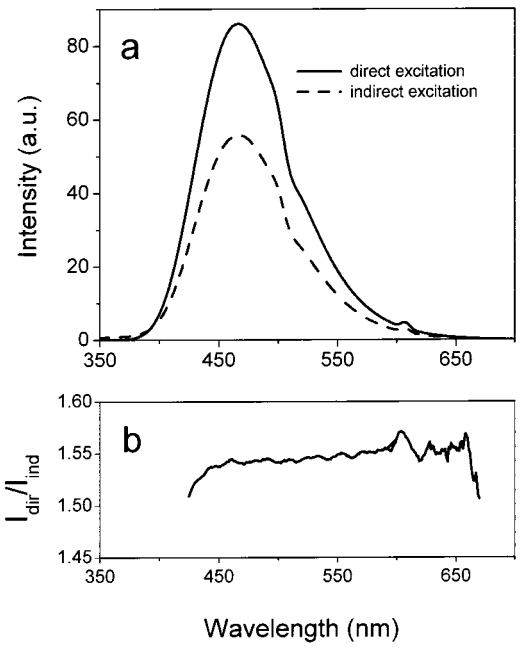

Figure 1. (a) Emission spectrum after excitation of 1-naphthol at pH = 6 (dashed line) and of the 1-naphtholate anion at pH = 12.5 (full line) both excited at the isosbestic point (302.5 nm). Due to rapid proton transfer (τ_p = 36 ps) only the anionic emission is observed at pH = 6.0 and in both cases the line shape is practically identical. (b) Graph showing that the intensity ratio of the two forms is independent of wavelength between 430 and 650 nm. The wavelength dependence below 430 nm is due to the residual acid fluorescence centered at 380 nm which exist at pH = 6.0. The "bumps" above 600 nm are due to the instrument.

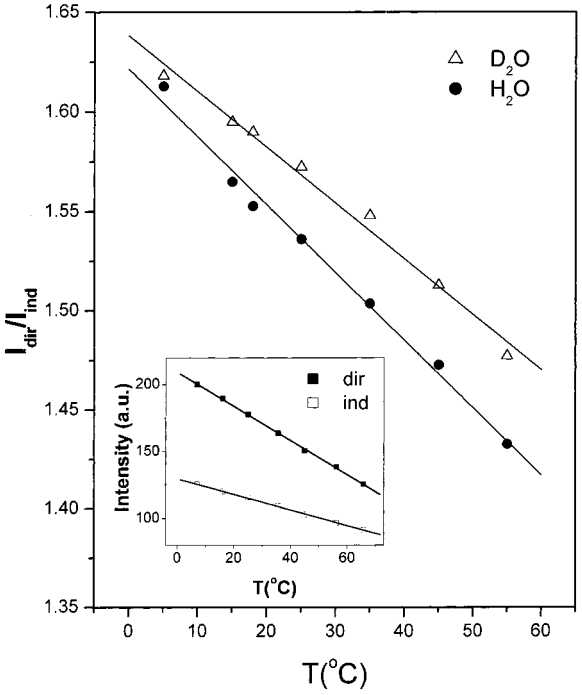

Figure 2. Ratio between fluorescence peak intensities of indirectly and directly excited naphtholate anion in H_2O and D_2O as a function of temperature. (Inset) Fluorescence intensities in H_2O of the directly excited (pH=12.5) and indirectly excited (pH=6.0) 1-naphtholate anion taken at the fluorescence peak (470 nm, uncorrected).

resolved using a high-sensitivity single-photon-counting detection system.[4] However, the detection of the self-quenching and the adiabatic geminate recombination reactions of 1-naphthol and its derivatives by time-resolved fluorescence techniques have remained a very demanding experimental task.[4,5] In comparison, steady-state fluorescence measurements can easily detect the small changes in the quantum-yield associated with the geminate quenching reaction (typically 10−40%) with better than 1% accuracy; however, such measurements lack dynamic resolution. For that reason, we have developed a theoretical method for estimating the on-contact self-quenching reaction rates of 1-naphtholate and its derivatives using steady-state fluorescence measurements at solution pH's where homogeneous quenching by bulk protons may be neglected during the lifetime of the excited state (pH ≥ 5.0).

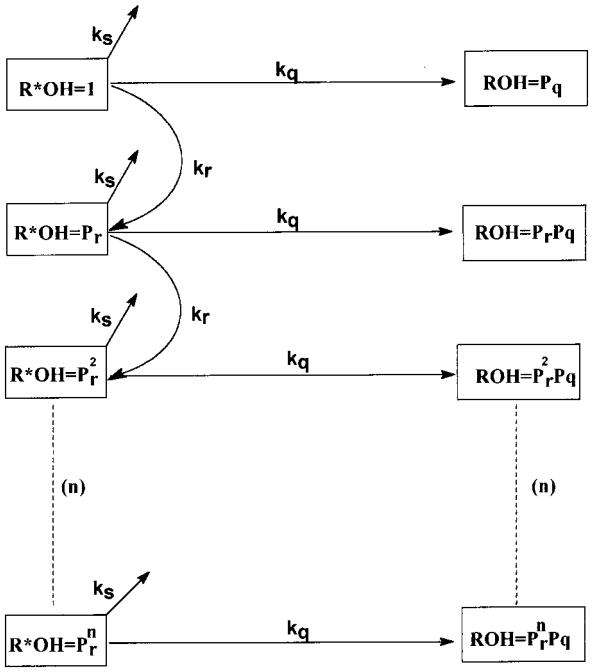

Figure 3. Schematic representation of the *n*-cycle reaction scheme of an electronically excited bound state (R*OH) which undergoes both reversible geminate−recombination reaction (k_r) and irreversible self-quenching reaction (k_q). k_s is the rate constant of escape of the pair to infinite mutual separation.

SCHEME 1

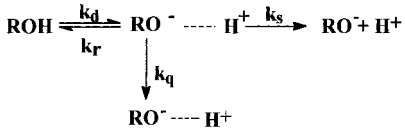

TABLE 1: Lifetimes of the Naphtholate Anion in H_2O and D_2O (pH (pD) =12.5) as a Function of the Temperature

T (°C)	H_2O (ns)	D_2O (ns)
5	8.56	25.08
15	8.29	24.14
18	8.21	23.60
25	7.98	22.55
35	7.77	22.36
45	7.50	21.34
55	7.18	20.46

***n*-Cycle Model of Coupled Reversible and Irreversible Geminate Recombination Reactions.** We analyze a general reversible dissociation reaction of an isolated ion pair[26] with an additional irreversible reaction on contact; see Scheme 1. The *n*-cycle reaction model is portrayed in Figure 3. RO···H^+, the contact reactant pair, may either disappear reactively (k_q and k_r represent the irreversible and reversible reaction rates, respectively) or disappear nonreactively by diffusion, which separates the isolated ion pair to infinite mutual distance (k_s).

Starting with an initial population of contact ion-pairs, at each reaction cycle the probability of irreversible quenching is P_q, the probability of ultimately separating by diffusion is P_s, and the probability of the pair to survive at the origin equals the probability, P_r, of back recombining to the bound state. The bound state then re-dissociates to initiate the next reaction cycle.

From the kinetic scheme we have,

$$P_q = \frac{k_q}{k_r + k_s + k_q},\ P_s = \frac{k_s}{k_r + k_s + k_q},\ P_r = \frac{k_r}{k_r + k_s + k_q} \quad (1)$$

The overall probability of the irreversible quenching reaction after n cycles is given by

$$\phi_q = P_q(1) + P_q(2) + P_q(3) + \cdots P_q(n) = \sum_1^n P_q(i) \quad (2)$$

where $P_q(i)$ is the probability of quenching in the ith reaction cycle.

Substituting ϕ_q for the geometric series in $P_q(i)$ one gets

$$\phi_q = P_q + P_r P_q + P_r^2 P_q + P_r^3 P_q + \cdots P_r^n P_q = \frac{P_q}{1 - P_r} \quad (3)$$

Substituting for P_r and P_q (eq 1), we finally get for the total yield of the irreversible quenching reaction

$$\phi_q = \frac{\dfrac{k_q}{k_r + k_s + k_q}}{1 - \dfrac{k_r}{k_r + k_s + k_q}} = \frac{k_q}{k_q + k_s} \quad (4)$$

The population of the bound state, ROH, after $n \rightarrow \infty$ cycles is given by

$$[\mathrm{ROH}]_{n\rightarrow\infty} = P_r^n = 0$$

Since for any finite k_r, $P_r < 1$.

The ultimate escape probability of the ion pair to form the free RO^- and H^+ ions, ϕ_s is given by

$$\phi_s = P_s + P_r P_s + P_r^2 P_s + \cdots + P_r^n P_s \quad (5)$$

$$\phi_s = \frac{P_s}{1 - P_r} = \frac{k_s}{k_s + k_q} \quad (6)$$

so $\phi_s + \phi_q = 1$ as it should be.

It follows from eq 4 that the total yield of the irreversible reaction in such a kinetic system is independent of k_r, the reversible geminate recombination rate of the contact pair. This is an interesting and important outcome of the reversibility of the on-contact recombination reaction; i.e., the reversible inner sphere recombination−dissociation process does not affect the total yield of the irreversible quenching reaction on the boundary of the inner sphere. ϕ_q and ϕ_s may be, thus, used as a convenient way for calculating k_q irrespective of the magnitude of k_r. The second constant appearing in eq 4 is the diffusion-limited rate constant of separation of the ion pair to infinity (or "escape"), k_s, which may be calculated from the physical properties of the solvent and solute using the steady-state solution of the diffusion equation

$$k_s = \frac{3DR_D}{a^3}\left(\exp\left(\frac{R_D}{a}\right) - 1\right)^{-1} \quad (7)$$

where D is the mutual diffusion coefficient between the ion pair, a is their contact radius, and R_D is the Debye length which scales the coulomb interaction,

$$R_D = \frac{|Z_1 Z_2| e^2}{\epsilon k_B T} \quad (8)$$

Here, Z_1 and Z_2 are the charge numbers of the two ions, e is the electron charge, ϵ is the static dielectric constant of the solvent, k_BT is the Boltzman factor, and $R_D = 7.1 \times 10^{-8}$ cm for 1:1 charges in water at 298 K. For the 1-naphtholate−H^+ pair, we have[5] $a = 5.5$ Å and $D = 10^{-4}$ cm^2 s^{-1}. We estimate the uncertainty in a and D to be less than 10% and 5%, respectively; this makes the total uncertainty in k_s less than 15%. Using these parameters, one gets $k_s = 4.8 \times 10^{10}$ s^{-1}.

Comparison of the *n*-Cycle Reaction Model to the Exact Numeric Solution of the Diffusion Equation. To compare between the simple, albeit exact, analytic predictions of the time-independent n-cycle reaction model and the exact numeric solution of the time-dependent diffusion equation, we have utilized the numeric algorithm that was used in our previous publication.[5] Briefly, the procedure of Agmon et al. for solving the spherical−symmetric Debye−Smoluchowski (SSDS) equation[9,25] was adjusted to include contact quenching.[5] Figure 4 shows the time behavior of the population of the ion pair using reaction parameters similar to that of the excited 1-naphthol−1-naphtholate system. In Figure 4, the ion pair is initially generated from the bound state and then is allowed to separate by diffusion while the residual population on contact remains reactive and either back recombines reversibly to form the initial bound state or disappears irreversibly by a parallel quenching reaction.

The different population curves were generated using a set of geminate recombination rate constants (k_r) while keeping all other parameters constant. As predicted by eq 6, all normalized population curves (the time-dependent escape probabilities, $[\phi_s]$, of the ion pair) converge at long times to a single ultimate survival value, $\phi_s(\infty)$, regardless of their different transient behavior at short times; see Figure 4a. The two limits of the reactions, $k_r \rightarrow 0$ and $k_r \rightarrow \infty$ are clearly realized in Figure 4. For $k_r \rightarrow 0$, the system approaches the irreversible quenching reaction limit with an apparent time transient given at long times by Hong and Noolandi[27]

$$[\phi_s]_t = \phi_s + Kt^{-1/2} \quad (9)$$

where K is a constant given by

$$K = \phi_s^2 \frac{a^2 k_q}{D(\pi D)^{1/2}} \exp(R_D/a) \quad (10)$$

When $k_r \rightarrow \infty$, the amplitude of the population transient goes to zero and the asymptotic long-time behavior of the escaped pair is delayed to longer and longer times due to the efficient trapping of the ion pair in its bound state. Figure 4b is a log−log plot of $[\phi_s]_t - \phi_s$ against time. It clearly shows that at long times all curves coalesce to a single-slope asymptote given by the $t^{-1/2}$ dependence predicted by eq 9. This shows not only the ultimate yield of quenching to be independent of the reversible recombination rate constant but also that the long-

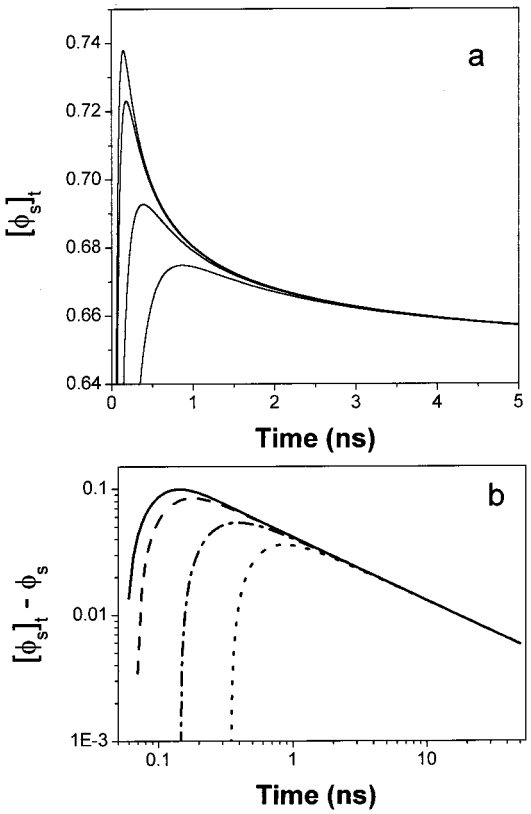

Figure 4. (a) Survival probability of an infinitely long-lived ion pair, $[\phi_s]_t$, which undergoes self-quenching reaction, following dissociation as a function of the reversible geminate recombination rate constant, k_r. Parameters used for the calculations are $D = 10^{-4}$ cm^2 s^{-1}, $R_D = 7$ Å, $a = 5$ Å, $k_d = 28 \times 10^9$ s^{-1}, $k_q = 3 \times 10^{10}$ s^{-1}; from top to bottom: $k_r = 0$, 2.3×10^{10} s^{-1}, 1.2×10^{11} s^{-1}, and 3×10^{11} s^{-1}. (b) log−log plot of $[\phi_s]_t - \phi_s$ as a function of time, using the same data set shown in part a. The solid line represents the $k_r = 0$ case. All the decay profiles coalesce at long times to a single slope of −0.5 as predicted by eq 9 in the text.

TABLE 2: Comparison of the Escape-Probability of 1-Naphtholate Anion Calculated by a Numeric Procedure and by Eq 6[a]

k_q (Å/ns)	ϕ_s (25 ns)	ϕ_s (50 ns)	ϕ_s (∞) (calcd)[b]	ϕ_s (∞) (analytic)[c]
0	1.000	1.000	1.000	1.000
10	0.903	0.902	0.900	0.900
50	0.648	0.646	0.642	0.642
500	0.156	0.155	0.152	0.152

[a] See text for details. [b] $\phi_s(\infty) = \phi_s(50\text{ ns}) - \int_{50\text{ns}}^{\infty} Kt^{-1/2}\,dt$; K is given by eq 10. [c] $\phi_s = k_s/(k_s + k_q)$.

time quenching yield is independent of k_r as well. This behavior was recently studied analytically by Gopich and Agmon.[22−24]

Table 2 compares the ultimate escape probability calculated analytically from eq 6 with numeric simulations similar to the ones shown in Figure 4 using an identical set of rate constants (k_d, k_r, k_s). The numeric calculations were carried out for 25 ns and for 50 ns, and the finite-time value, ϕ_s (50 ns) was corrected analytically to infinite times by integrating eq 9 from 50 ns to infinity. The numeric value of $\phi_s(\infty)$ was found to be identical to the third decimal point to the result of the analytic *n*-cycle reaction model, eq 6. For further applications, the accuracy of the numeric calculation was judged to be adequate when the calculation was truncated after 50 ns following the initial creation of the bound state.

Analysis of the Excited-State Acid−Base Dynamics of 1-Naphthol using the *n*-Cycle Reaction Model. Equations 1−6 are exact for ground-state reactions where the lifetimes of the bound and the unbound states are infinite. For excited-state reactions, the lifetimes of the bound and unbound states are finite and the ultimate survival probability of the pair in the excited state becomes zero.

SCHEME 2

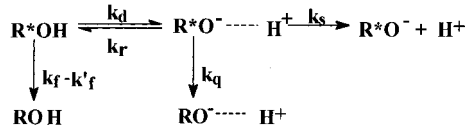

Below, we show that for the electronically excited 1-naphthol system one can use the simple form of eq 6 in combination with the quantum-yield ratio Q_{dir}/Q_{ind} and calculate the corresponding k_q values to within 10−20% of the exact numeric calculations. Several algebraic approximations are involved in the analytical calculation of k_q, but neither of them is severe as long as the lifetimes of the acid and base forms in the excited state are relatively long; i.e., k_f and $k'_f \ll k_d$, k_r, k_q, and k_s. Where $(k_f)^{-1}$ and $(k'_f)^{-1}$ are the excited-state fluorescence lifetimes of the acid (bound state) and base (ion-pair state) forms, respectively. These conditions are met for 1- naphthol and its derivatives where k_f and k'_f are typically about 10^8 s^{-1} and all other kinetic parameters are about 2 orders of magnitude larger.

We start the analysis of the excited-state 1-naphthol system by the *n*-cycle reaction model by observing that the absolute excited-state quantum yield of the 1- naphtholate anion (base) is given by

$$Q = k'_0 \int_0^{\infty} [\phi^*_s]_t dt \tag{11}$$

where k'_0 is the purely radiative decay rate of the base and $[\phi^*_s]_t$ is the time-dependent survival probability of the naphtholate ion in the excited state. $[\phi^*_s]_t$ may be written as

$$[\phi^*_s]_t = [\phi'_s]_t \exp(-k'_f t) \tag{12}$$

where $[\phi'_s]_t$ is the time-dependent survival probability of the naphtholate anion in the unbound-state decaying time frame.

Scheme 2 describes a coupled reversible−irreversible geminate recombination reactions between a bound and unbound state having finite excited-state lifetimes, τ_f and τ'_f, respectively. Scheme 2 is drawn in the unbound-state (base) decaying time frame.

ϕ'_s, the (time-independent) ultimate escape probability in the electronically excited base time frame, may now be calculated with the *n*-cycle summation procedure:

$$\phi'_s = P_d P_s + P_r P_d^2 P_s + \cdots + P_r^{n-1} P_d^n P_s = P_s \sum_{i=1}^{n} P_r^{i-1} P_d^i \tag{13}$$

$$\phi'_s = \frac{P_d P_s}{1 - P_d P_r} = \frac{P_s}{\frac{1}{P_d} - P_r} \tag{14}$$

where

$$P_d = \frac{k_d}{k_d + k_f - k'_f},\ P_r = \frac{k_r}{k_r + k_s + k_q},\ P_s = \frac{k_s}{k_r + k_s + k_q},\ P_q = \frac{k_q}{k_r + k_s + k_q} \tag{15}$$

P_d is the dissociation probability and all other symbols have the meaning of the text.

Substituting in eq 14, we have

$$\phi'_s = \frac{\dfrac{k_s}{k_r + k_s + k_q}}{\dfrac{k_f - k'_f + k_d}{k_d} - \dfrac{k_r}{k_r + k_s + k_q}} = \frac{k_s}{k_s + k_q + (k_r + k_s + k_q)\left(\dfrac{k_f - k'_f}{k_d}\right)} \quad (16)$$

We notice that the overall dissociation lifetime, τ_{off}, is given by

$$\tau_{off} = \frac{1}{k_d P_s} = \frac{k_r + k_q + k_s}{k_s k_d} \quad (17)$$

so,

$$\phi'_s = \frac{k_s}{k_s + k_q + k_s \tau_{off}(k_f - k'_f)} \quad (18)$$

Equation 18 is identical to the expression given elsewhere[22,23] using much more elaborated procedures. For $k_d \gg (k'_f - k_f)$ and $k_r \leq (k_s + k_q)$, eq 16 is reduced to $\phi'_s \approx k_s/(k_s + k_q) = \phi_s$. So in these conditions ϕ'_s is roughly independent of k_r, similar to a ground-state situation ($\phi'_s = \phi_s$ in the special case when $k'_f = k_f$, including the trivial ground-state case $k'_f = k_f = 0$).

Finally, Pines and Fleming have shown that $[\phi'_s]_t$ is well approximated by the long-time behavior of the irreversible quenching reaction.[4] Integrating $[\phi'_s]_t$ over time, they have come out with an approximate analytic expression for ϕ'_s using readily observable steady-state quantum-yield parameters:

$$\phi'_s \approx \frac{Q_{ind}}{Q_{dir}} - K(\pi k'_f)^{-1/2} \quad (19)$$

where K is the constant given by eq 10. The term in eq 19 which depends on K describes the contribution of the population of the naphtholate anion which undergoes rapid contact quenching to the total quantum yield of the naphtholate anion. This contribution of the quenched population to the total quantum yield is usually very small (it is assumed to be zero at the so-called "static" quenching limit) compared to the contribution of the unquenched population, and in the case of 1-naphthol, it is only about 3% using K (25 °C) $= 1.6 \times 10^{-6}$ s$^{1/2}$.[4] We thus conclude that the $K-$term in eq 19 may be neglected altogether in the case of 1-naphthol and that a simple relation, $\phi'_s \approx Q_{ind}/Q_{dir}$, between the excited-state escape probability and the measured steady-state quantum yields ratio, holds within reasonable error bars (about $\pm 10-15\%$; see below).

Table 3 summarizes the experimental findings. The calculation of the quantum yield of the naphtholate anion was carried out using the numeric simulation of the naphtholate decay up to 50 ns following its initial creation. The numeric procedure was carried out using the finite lifetimes of the naphtholate anion (Table 1) and the naphthol acid (4.5 ns) as additional reaction parameters.[5] k_r was held constant at its room-temperature value as the total area under the simulated decay curve is practically independent of k_r; simulating the decay curves with a 25-fold change in k_r around its room-temperature value using $k_r = 3 \times 10^9$s^{-1} and $k_r = 8 \times 10^{10}$ s^{-1} (about 15 times the variation found in $k_q(T)$ in the temperature range studied) resulted in less than 0.8% total change in the area under the decay curve. The area under the decay curve (the absolute quantum yield) was then fitted to the experimentally measured quantum yield, with k_q used as the only fitting parameter in the program. All reaction parameters were taken from the literature (see footnotes to Table 3). k_d was not varied in our simulation. Under our approximation, k_d has no effect on ϕ'_s as long as $(k_d)^{-1}$ is very short compared to the fluorescence lifetimes of the 1-naphthol and the 1-naphtholate molecules. In actuality, the error associated with this assumption is less than 1%. For the analytic calculations, we used the time-independent expression as described in the text:

$$\phi'_s \approx \frac{k_s}{k_s + k_q} \approx \frac{Q_{ind}}{Q_{dir}} \approx \frac{I_{ind}}{I_{dir}}$$

or

$$k_q \approx k_s\left(\frac{I_{dir}}{I_{ind}} - 1\right) \quad (20)$$

k_s was calculated using eq 7 with reaction parameters identical to those used in the numeric fit (Table 4). A comparison between the analytic and numeric methods reveals the simple analytic procedure to be as informative as the numeric one, the difference between the two sets of quenching constants being almost constant and small; $2-5\%$ in the case of 1-naphthol in H_2O and $10-12\%$ in the case of 1-naphthol in D_2O. In comparison with the full kinetic analysis of the time-resolved decay profiles of both 1-naphthol and 1-naphtholate,[5] the absolute values of the quenching reaction at 25 °C were about 20% and 10% lower for H_2O and D_2O, respectively. These differences are much smaller than the overall uncertainty in determining the absolute

TABLE 3: Intensity Ratios I_{ind}/I_{dir} and On-Contact Quenching Rate Constants of 1-naphtholate Following Its Photodissociation in H_2O and D_2O

T (°C)	I_{ind}/I_{dir}		$k_q \times 10^{-10}$ (s^{-1})[a,b]		$k_q(H_2O)^{a}/k_q(D_2O)$	$k_q \times 10^{-10}$ (s^{-1})[b,c]		$k_q(H_2O)^{c}/k_q(D_2O)$
	H_2O	D_2O	H_2O	D_2O		H_2O	D_2O	
5	1.613	1.618	2.12	1.29	1.64	2.02	1.44	1.40
15	1.565	1.595	2.42	1.59	1.52	2.33	1.76	1.32
18	1.553	1.590	2.47	1.66	1.49	2.42	1.85	1.31
25	1.536	1.572	2.71	1.87	1.45	2.62	2.06	1.27
35	1.503	1.548	2.98	2.12	1.41	2.91	2.34	1.24
45	1.473	1.513	3.22	2.28	1.41	3.15	2.54	1.24
55	1.433	1.478	3.31	2.39	1.38	3.25	2.69	1.21

[a] Numeric calculation using the SSDS program.[5,9,25] [b] $a = 5.5$ Å, $k_r = 2.7 \times 10^{10}$ s^{-1}, $k_d(H_2O) = 27.8 \times 10^9$ s^{-1}, $k_d(D_2O) = 7.14 \times 10^9$ s^{-1}. [c] Calculated from eq 20.

TABLE 4: Reaction Parameters Used for Calculating Quenching Rates in H_2O and D_2O

T (°C)	ϵ_s		R_D (Å)		$D \times 10^5$ (cm^2 s^{-1})	
	D_2O[a]	H_2O[b]	D_2O[c]	H_2O[c]	D_2O[d]	H_2O[d]
5	85.76	85.48	6.99	7.01	4.73	6.73
15	81.95	81.62	7.05	7.08	6.05	8.47
18	80.84	80.49	7.10	7.12	6.46	9.00
25	78.30	77.93	7.13	7.16	7.45	10.1
35	74.82	74.42	7.21	7.25	8.92	12.1
45	71.5	71.08	7.30	7.35	10.4	14.1
55	68.35	67.89	7.40	7.45	12.0	16.1

[a] Previously published.[31] [b] Previously published.[32] [c] Calculated from eq 8. [d] Calculated using $D = D_{naphtholate} + D_{H+}$ with D calculated from conductivity data; $D = RT\lambda/|z|F^2$, λ_{H+}, and λ_{D+} were taken from earlier work[33] and assume $D_{naphtholate} = k_B T/6\pi\eta a$. η values were taken from earlier work.[34]

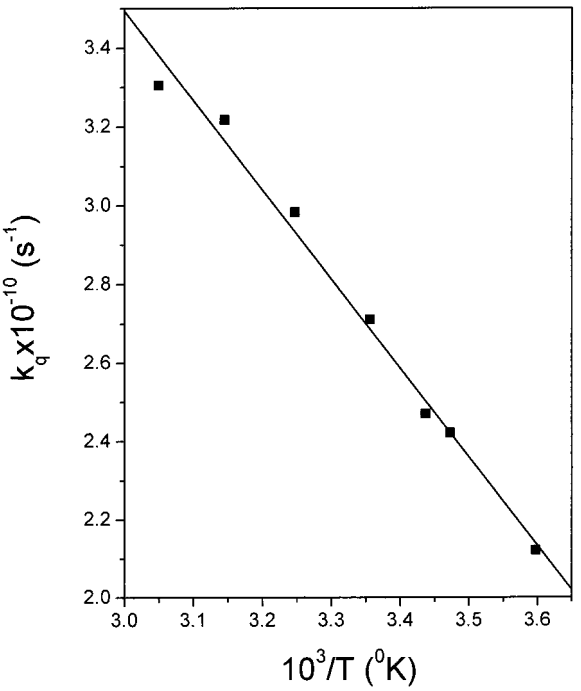

Figure 5. Arrhenius plot of k_q in H_2O against the reciprocal absolute temperature. $E_a = 1.8$ kcal/mol.

values of k_q from extremely demanding time-resolved measurements and analyzing the time-resolved data with the spherical-symmetric diffusion equation in a multiparameter fit while applying a continuum interaction model. We conclude that relatively simple quantum-yield measurements are proven to be very useful in predicting the magnitude of the on-contact quenching rate constant of 1-naphtholate following its photodissociation. In future experiments, this procedure may be utilized to estimate k_q directly from the steady-state measurements via eq 20. This considerably simplifies the complex and time-consuming experimental and numeric procedures involved in the time-resolved measurements and avoids the tedious curve-fitting procedures.[25] Our analysis also provides, in combination with simple steady-state fluorescence measurements, a general method for the detection and estimation of the self-quenching rate constant of many 1-naphthol derivatives, which exhibit kinetic features similar to the parent 1-naphthol molecule.

Temperature Dependence of k_q. In Figure 5, $k_q(H_2O)$ calculated by the numeric procedure (Table 3) was plotted against the reciprocal temperature. At 25 °C, the activation energy, E_a, was found to be 1.8 and 2.4 kcal/mol for H_2O and D_2O solvents, respectively. The frequency factor was about 10^{12} s^{-1} for the two solvents. These observations and the magnitude of the isotope effect, $k_q(H_2O)/k_q(D_2O) = 1.4 \pm 0.1$ at 25 °C, are consistent with a proton-transfer process in water which is nearly activationless on the proton coordinate and has a small activation barrier which originates from the solvent bath. In Figure 6a, k_q is plotted against the diffusion coefficient of H^+ and D^+. The two sets of diffusion coefficients tend to correlate linearly with k_q in the relatively narrow range of temperatures used in our experiment. To show that this is not a unique correlation, we have used a semiempirical relation describing the quenching reaction rate as a solvent-dependent frequency factor times an activation factor:[28]

$$k_q = W_s \exp(-E_a/RT) \tag{21}$$

where W_s is a solvent-dependent prefactor. Equation 21 is

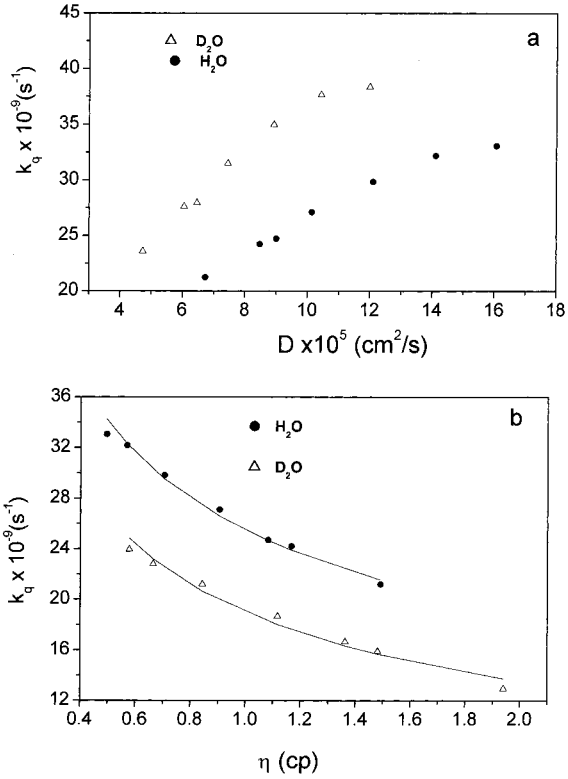

Figure 6. (a) On-contact quenching rate (k_q) plotted against the mutual proton−anion diffusion coefficient in the temperature range of 5−55 °C. (b) On-contact quenching reaction rate (k_q) plotted against solvent viscosity. The solid lines are the data fit using eq 22.

formally identical with a thermally activated barrier crossing process.[29] As it is not clear what is the actual mechanism of the quenching reaction,[19,4] we have chosen a form of eq 21 which uses an empirical relation motivated by Kramers' theory[30]

$$k_q = \frac{B}{\eta^{\beta}} \exp(-E_a/RT) \tag{22}$$

where η is the solvent viscosity, and β and B are parameters to be determined by the best-fit procedure. The motivation for using η as a fitting parameter stems from the observation that the isotope effect on k_q, $k_q(H_2O)/k_q(D_2O)$, appears to be independent of η and was found to be 1.32 ± 0.03 when k_q was plotted against η, Figure 6b. A fit of $k_q(H_2O)$ by eq 22 yielded $B = 2.55 \times 10^{10}$ (cp, s^{-1}), $\beta = 0.42$, and $E_a \approx 0$. A similar fit of $k_q(D_2O)$ yielded $B = 1.90 \times 10^{10}$ (cp, s^{-1}), $\beta = 0.49$, and $E_a \approx 0$, with an isotope effect in B, $B_{H+}/B_{D+} = 1.34$. The parameters of the fit demonstrate once more that the on-contact quenching process is nearly activationless on the proton reaction coordinate. They also show the formal dependence on the solvent viscosity to be fractional. Interestingly, the magnitude of β, the fractional factor, is similar to the ones found in several nonradiative rate processes.[30]

Conclusion

The on-contact quenching rate of 1-naphtholate by its geminate proton following the photodissociation of 1-naphthol was found to be temperature-dependent with a small activation energy of about 1.8 kcal/mol in H_2O and with a small isotope effect of 0.6 kcal/mol. The reaction parameters point toward a reaction, which is mediated on-contact by the solvent, although it is not yet understood by what mechanism. In this respect, the identification of an efficient proton self-quenching reaction

following the photodissociation of 1-naphthol has not solved the general problem of elucidating the various quenching mechanisms of 1-naphthol and the 1-naphtholate anion.[4,19] Additional kinetic data on the quenching reaction of 1-naphthol and its derivatives is clearly needed before this question may be resolved. Such additional kinetic data may be easily obtained by the procedure outlined in this study.

Acknowledgment. The authors acknowledge E. B. Krissinel and N. Agmon for the use of the SSD program. This work was supported in part by James Franck German−Israel Binational Program for Laser-Matter Interaction.

References and Notes

(1) Onsager, L. *J. Chem. Phys*. **1934**, *2*, 599.
(2) Mozumder, A. *J. Chem. Phys*. **1968**, *48*, 1659.
(3) Pines, E.; Huppert, D. *J. Chem. Phys*. **1986**, *84*, 3576.
(4) Pines, E.; Fleming, G. R. *Chem. Phys*. **1994**, *183*, 393.
(5) Pines, E.; Tepper, D.; Magnes, B. Z.; Pines, D.; Barak, T. *Ber. Buns. Phys. Chem*. **1998**, *102*, 504.
(6) Ireland, J. F.; Wyatt, P. A. H. *Adv. Phys. Org. Chem*. **1976**, *12*, 131.
(7) Weller, A. *Prog. React. Kinet*. **1961**, *1*, 187.
(8) Robinson, G. W.; Thistlethwaite, J.; Lee, J. *J. Phys. Chem*. **1991**, *95*, 10448.
(9) Pines, E.; Huppert, D.; Agmon, N. *J. Chem. Phys*. **1988**, *88*, 5620.
(10) Pines, E.; Fleming, G. R. *J. Phys. Chem*. **1991**, *95*, 10448.
(11) Rosenberg, J. L.; Brinn, I. *J. Phys. Chem*. **1972**, *76*, 3558.
(12) Harris, C. M.; Selinger, J. *J. Phys. Chem*. **1980**, *84*, 1366.
(13) Webb, S. P.; Yeh, S. W.; Phillips, L. A.; Tolbert, L. M.; Tolbert, M. A.; Clark, J. H. *Abstr. Pap. Am. Chem. Soc*. **1984**, *188*:116-Phys.
(14) Webb, S. P.; Phillips, L. A.; Yeh, S. W.; Tolbert, L. M.; Clark, J. H. *J. Phys. Chem*. **1986**, *95*, 5154.
(15) Lee, J.; Robinson, G. W.; Webb, S. P.; Phillips, L. A.; Clark, J. H. *J. Am. Chem. Soc*. **1986**, *108*, 6538.
(16) Shizuka, H.; Ogiwara, T.; Narita, A.; Sumitani, M.; Yoshihara, K. *J. Phys. Chem*. **1986**, *90*, 6708.
(17) Krishman, R.; Fillingim, T. G.; Lee, J.; Robinson, G. W. *J. Phys. Chem*. **1990**, *112*, 1353.
(18) Agmon, N.; Huppert, D.; Massad, A.; Pines, E. *J. Phys. Chem*. **1991**, *95*, 10407.
(19) Martynov, Yu.; Zaitsev, N. K.; Soboleva, V.; Uzhinov, B. M.; Kuz'min, M. G. *Zh. Prik. Spectrosc*. **1978**, *28* (6), 1075.
(20) Förster, T. *Z. Elektrochem*. **1950**, *54*, 531.
(21) Weller, A. *Z. Elektrochem*. **1952**, *56*, 662.
(22) Gopich, I. V.; Solntsev, K. M.; Agmon, N. *J. Chem. Phys*. **1999**, *110* (4), 2164.
(23) Agmon, N. *J. Chem. Phys*. **1999**, *110* (4), 2175.
(24) Agmon, N.; Gopich, I. V. *J. Chem. Phys*. **1999**, *110* (21), 10433.
(25) Krissinel, E. B.; Agmon, N. *J. Comput. Chem*. **1996**, *17*, 1085.
(26) Eigen, M. *Angew. Chem., Int. Ed. Engl*. **1964**, *3*, 1.
(27) Hong, K. M.; Noolandi, J. *J. Chem. Phys*. **1978**, *68*, 11.
(28) Borgis, D.; Hynes, J. T. *J. Phys. Chem*. **1996**, *100*, 1118.
(29) Pines, E.; Magnes, B. Z.; Lang, M. J.; Fleming, G. R. *Chem. Phys. Lett*. **1997**, *281*, 413.
(30) Courtney, S. H.; Fleming, G. R. *J. Chem. Phys*. **1985**, *83*, 215.
(31) Dean, J. A. *Lange's Handbook of Chemistry*; McGraw-Hill: New York, 1973; Vol. 5, p 170.
(32) Malmberg, G.; Maryott, A. *Res. Nat. Bur. Stand*. **1950**, *56*, 1.
(33) Baumann, E. W. *J. Chem. Eng. Data* **1993**, *38*, 12.
(34) Kazavchinscii, Y. Z. *Heavy Water: Thermophysical Properties*; Israel Program For Scientific Translations: Jerusalem, 1971.